Venus tesserae feature layered, folded, and eroded rocks

Paul K. Byrne[1], Richard C. Ghail[2], Martha S. Gilmore[3], A. M. Celâl Şengör[4], Christian Klimczak[5], David A. Senske[6], Jennifer L. Whitten[7], Sara Khawja[8], Richard E. Ernst[8,9], and Sean C. Solomon[10]

[1]*Planetary Research Group, Department of Marine, Earth, and Atmospheric Sciences, North Carolina State University, Raleigh, NC 27695, USA*

[2]*Department of Earth Sciences, Royal Holloway, University of London, Egham, TW20 0EX, UK*

[3]*Earth and Environmental Sciences, Wesleyan University, Middletown, CT 06459, USA*

[4]*Eurasia Institute of Earth Sciences and Department of Geology, Faculty of Mines, Istanbul Technical University, 34469 Ayazağa, İstanbul, Turkey*

[5]*Department of Geology, University of Georgia, Athens, GA 30602, USA*

[6]*Jet Propulsion Laboratory, California Institute of Technology, Pasadena, CA 91109, USA*

[7]*Department of Earth and Environmental Sciences, Tulane University, New Orleans, LA 70118, USA*

[8]*Department of Earth Sciences, Carleton University, Ottawa, ON K1S 5B6, Canada*

[9]*Faculty of Geology and Geography, Tomsk State University, Tomsk, 634050, Russia*

[10]*Lamont-Doherty Earth Observatory, Columbia University, Palisades, NY 10964, USA*

ABSTRACT

Tesserae on Venus are locally the stratigraphically oldest units preserved on the planet. Morphological, spectroscopic, and geophysical measurements support the possibility that tessera blocks are the equivalent on Venus to felsic continental crust on Earth. These units are characterized by pervasive tectonic deformation that includes normal faults, graben, thrust faults, and folds. In several tesserae, a set of (often highly) curved, parallel lineaments is also present. These lineaments strongly resemble layered volcanic or sedimentary sequences on Earth having arcuate or sinuous outcrop patterns that follow undulating topography. Should this analogy hold for Venus, then these outcrop patterns imply some erosion of the tessera units in which these strata occur; the radar-dark materials filling proximal lows might be deposits of that eroded material. We recognize this outcrop pattern in geographically dispersed tessera units, so the preservation of interior layering could be common for this terrain type. If so, then tesserae may correspond to the igneous and sedimentary cover atop continents on Earth.

INTRODUCTION

Tessera terrain on Venus is characterized by numerous sets of intersecting tectonic features, interpreted as mixes of extensional and shortening structures that record complex strain histories for individual exposures (e.g., Barsukov et al., 1986; Ghent and Hansen, 1999). Indeed, tessera units boast styles of deformation not observed on any other planetary body (aside, perhaps, from the ancient continental interiors on Earth). Tessera terrain occupies 7.3% of the Venus surface and locally is always stratigraphically older than surrounding plains units (e.g., Ivanov and Head, 2011). Tessera units occur as both large plateaus thousands of kilometers across and as smaller

inliers—isolated, high-standing regions hundreds of kilometers in horizontal extent that are embayed by younger volcanic deposits (Ivanov and Head, 2011).

One hypothesis for tessera formation is that the surficial material is basaltic and was the cooling crust of a voluminous subsurface magma pond (e.g., Hansen, 2006). Another view is that tesserae may be the Venus counterparts of continents on Earth, on the basis of morphology, gravity anomaly signature, and inferred composition (e.g., Hashimoto et al., 2008; Romeo and Capote, 2011). Indeed, data from the Galileo and Venus Express (VEx) missions suggest that the surfaces of tesserae may be compositionally distinct from much of the rest of the Venus surface (Helbert et al., 2008). For example, surface emissivity data from the Visible and Infrared Thermal Imaging Spectrometer (VIRTIS) instrument on VEx provide evidence that the Alpha Regio tessera is more felsic than adjacent basaltic plains (Gilmore et al., 2015). Although fractional crystallization can yield felsic rocks from mafic magma, the high volume ratio of mafic to felsic melts would challenge such an origin for tessera terrain if the composition of the materials comprising tessera at the surface represented that of the full column of underlying crust (e.g., Gilmore et al., 2017). These arguments are consistent with the hypothesis that tesserae are analogous to granitic continental materials on Earth, which form via crustal recycling in the presence of substantial volumes of water (e.g., Campbell and Taylor, 1983).

INTERIOR LAYERING

When resolved with Magellan synthetic aperture radar (SAR) left- and right-looking global radar mosaics, which have a spatial resolution of 75 meters per pixel (m/px), there is evidence for sets of curved, parallel lineaments (Senske and Plaut, 2000, 2009) in addition to the recognized extensional and shortening structures within tesserae. For example, within Tellus Tessera, an

exposure of this terrain type at mid-northern latitudes in Venus' eastern hemisphere, sub-parallel, radar-bright lineaments appear to follow local changes in topography and can be traced continuously for tens of kilometers (Fig. 1). Where these linear features strike approximately perpendicular to the radar look direction, their spacing decreases, which likely reflects radar foreshortening (a distortion common in radar images of mountainous terrain facing the SAR antenna that results in slopes appearing steeper in map view than they really are).

On the basis of Magellan radar image resolution, these candidate strata are ~100–200 m thick, although fainter lineaments that parallel the more prominent examples suggest that thinner layers, perhaps tens of meters thick, are also present. In addition to those examples within Tellus Tessera (Senske and Plaut, 2000, 2009), we have identified this curvilinear outcrop pattern in Ovda Regio (Fig. 2A) and Alpha Regio (Fig. 2B) tesserae, as well as in Manatum Tessera (e.g., at 8°S, 67°E) and Thetis Regio tessera (e.g., at 11°S, 130°E).

These lineaments bear a strong morphological resemblance to strata in layered sequences on Earth that have an arcuate or sinuous outcrop pattern from having been exposed by erosion on the flanks of ridges or valleys (Fig. 2C). The irregular, curvilinear patterns of these lineaments in tesserae may thus, by analogy, be indicative of exposed layers that follow undulating ridge-and-trough topography with length scales of tens of kilometers.

The nature of these strata is unclear, although they could be volcanic or sedimentary units. If sedimentary, the lithology of such units is difficult to ascertain. Under current Venus surface conditions at typical elevations (~740 K and 9.3 MPa), there is no means by which fluvial or shallow marine sediments could form, and carbonate rocks are not thermodynamically stable (e.g., Fegley and Treiman, 1992). The atmosphere is well capable of transporting sediment (Greeley et al., 1984), but few definitive aeolian landforms and deposits have been recognized in

Magellan data, and most of those are associated with impact ejecta (Craddock, 2011). Water-derived sedimentary rocks might perhaps have formed under different environmental conditions from those that prevail today, particularly if the Venus climate was once more clement (e.g., Way and Del Genio, 2020). Without in situ chemical analyses and high-resolution images of tessera rocks, however, such inferences are difficult to test.

Explosive volcanism on Venus today is generally thought to be inhibited by the high surface pressure (e.g., Head and Wilson, 1986), although at least two likely candidate pyroclastic deposits have been identified (Ghail and Wilson, 2015; Campbell et al., 2017). Alternatively, the tessera layers could be stacked lava flows (i.e., trap terrain) of mafic or felsic composition (Gilmore et al., 2015). Up to 70% of the planet's surface is occupied by plains lavas (Ivanov and Head, 2011), and widespread (if episodic) volcanism is likely responsible for the average model crater age of the Venus surface of 700–800 Myr (McKinnon et al., 1997). If the layers are lava traps, then tesserae represent substantial accumulations of effusive flows akin to large igneous provinces (LIPs) on Earth, e.g., the mafic Deccan or Siberian traps (in India and Russia, respectively), or silicic LIPs (SLIPs) such as the Sierra Madre Occidental in Mexico (Ernst, 2014).

FOLDING OF TESSERAE

Whatever the composition(s) of the tesserae, folding helps to explain the map patterns we observe. Both short- and long-wavelength folds have been widely seen in tesserae (e.g., Ghent and Hansen, 1999; Romeo and Capote, 2011; Cofrade et al., 2019). Horizontal shortening of tessera units (or the precursor rocks) is predicted to yield periodic fold trains of antiforms and synforms (possibly featuring flexural slip along the interfaces of any interior layers). Under this

scenario, internal strata should dip away from ridges and toward the troughs, but neither Magellan altimetric (Ford and Pettengill, 1992) nor stereo-derived (Herrick et al., 2012) topographic data (with horizontal resolutions of 4.6 km/px and 0.6 km/px, respectively) are of sufficient resolution to measure reliably the dip angles of the lineaments we interpret as exposed layers.

Nonetheless, under the assumption that these ~10-km-scale ridges and valleys are indeed upright antiforms and synforms, we estimate the shortening they represent by assessing with stereo-derived topography the geometry of ridges and valleys along two ~400-km-long transects, one each in Tellus Tessera (from 36.8°N, 78.6°E to 40.6°N, 78.0°E) and Ovda Regio (from 6.9°S, 82.3°E to 3.3°S, 82.2°E). We approximate each assumed fold limb as a triangle, such that the horizontal shortening strain is $\Delta L = L_{final} - L_{initial}$, where L is length, $L_{final} = \lambda/4$, $L_{initial} = [(\lambda/4)^2 + a^2]^{0.5}$, λ is fold wavelength, and a is fold amplitude. With wavelengths of 10–20 km and amplitudes of 200–300 m, these are gentle folds with interlimb angles of ~175° that likely represent shortening strains of only ~0.2–0.5%, a finding consistent with earlier work (e.g., Ghent and Hansen, 1999).

Folding also accounts for distinctive lenticular features that occur widely within tesserae, such as the examples in Fig. 3A. These features morphologically resemble eroded periclinal folds, i.e., folds with double-plunging fold axes. Periclines are common within major shortening systems on Earth, such as in Iran's Zagros Mountains (Molinaro et al., 2005), in southern China (Li et al., 2016), and in the Sulaiman Range of Afghanistan and Pakistan (Reynolds et al., 2015) (Fig. 3B). Given that the tesserae were formed at least in part by horizontal convergence (e.g., Romeo and Capote, 2011), it would perhaps not be surprising were such folds present on Venus. The "circular troughs" discussed by Cofrade et al. (2019), and attributed by those authors to local

diapirism, may also be eroded periclinal folds. Further, polyphase deformation can readily generate complex fold interference patterns (Ramsey, 1967) and has been invoked, for instance, to account for the "basin-and-dome" topography at the center of Alpha Regio (Hansen and Willis, 1996).

EROSION OF TESSERAE

The arcuate map patterns of tessera lineaments are consistent with gently dipping or near-horizontal layers. Yet even with horizontal shortening sufficient to produce folds with amplitudes as great as 500 m (as for the example in Fig. 1), some erosion is required to expose the constituent strata of layered tesserae and so account for outcrop patterns that follow local topography, as well as generate the eroded periclines postulated above.

The prospect for erosion on Venus is equivocal, especially given the apparent dearth of aeolian deposits on the planet (Craddock, 2011). Yet some transport of fine materials by wind takes place on Venus. For instance, sand-sized particles were seen to be removed from the Venera 13 lander over about an hour, with wind the most likely cause of movement (Selivanov et al., 1982). Even a very low wind erosion rate—for instance, 10^{-6} m yr^{-1}, comparable to the sedimentation rate on the North Atlantic abyssal plain (Carvalho et al., 2011)—will remove 700–800 m of material over the average model age for the planet's surface (McKinnon et al., 1997). Given that tesserae tend to be the stratigraphically oldest units where they are observed, they are likely to have been subjected to aeolian erosive action for the greatest amount of time of any portion of the currently exposed surface of Venus.

Erosion of tessera therefore provides a means for the exposure of layered units within this terrain type. Erosion also presents another explanation for the radar-dark materials (e.g., those

marked by blue arrows in Figs. 1A, 2A, 2B, and 3A) that fill local lows in tesserae and are commonly interpreted as volcanic (e.g., Ivanov, 2001). Some of these materials might instead be sediments, sourced from tessera rocks, that are fine-grained at the Magellan radar wavelength (12.6 cm) and thus have low backscatter. If so, these radar-dark units may more closely resemble the layered strata observed at the Venera 13 and 14 landing sites (Basilevsky et al., 1985).

CONCLUSIONS AND OUTLOOK

There is morphological evidence for layers within numerous tessera units on Venus. The nature and attitude of these strata remain unclear. They might be lava traps or sedimentary formations; they may be horizontal or gently folded; they may have formed after Venus experienced a runaway atmospheric greenhouse (Ingersoll, 1969), or they may date from an earlier, more temperate climate (Way and Del Genio, 2020). But given their widespread occurrence, such interior strata could be common to tesserae. The presence and map patterns of internal layering denotes a complex formational history for these enigmatic units that includes volcanic and/or sedimentary deposition, at least one phase of folding, and exhumation by some erosive action (Fig. 4).

Layered units are not compatible with interpretations of exposed tesserae as outcrops of crystalline basement. However, layered tesserae, whether mafic or felsic, do not preclude a continental crust-like basement—only that such rock is not exposed where layered material is present. Continental interiors on Earth frequently feature sedimentary cover. Moreover, tesserae are identified on the basis of morphology, but there is no requirement that this terrain type represents everywhere the same lithology or is the product of a single formational or deformational history (cf. Hansen and Willis, 1996). Our finding of layering within tesserae,

178 therefore, does not rule out the possibility that they are the Venus counterparts to continents on
179 Earth (Hashimoto et al., 2008; Romeo and Capote, 2011). A fuller understanding of the nature of
180 these units must await high-resolution radar or optical imaging and in situ chemical assessment
181 by future orbiter and landed missions.
182
183 **ACKNOWLEDGMENTS**
184 This research made use of NASA's Planetary Data System and Astrophysics Data System.
185
186 **REFERENCES CITED**
187 Barsukov, V. L., et al., 1986, The geology and geomorphology of the Venus surface as revealed
188 by the radar images obtained by Veneras 15 and 16: Journal of Geophysical Research, v. 91,
189 p. D378–D398, https://doi.org/10.1029/JB091iB04p0D378.
190 Basilevsky, A. T., Kuzmin, R. O., Nikolaeva, O. V., Pronin, A. A., Ronca, L. B., Avduesvsky, V.
191 S., Uspensky, G. R., Cheremukhina, Z. P., Semenchenko, V. V., and Ladygin, V. M., 1985,
192 The surface of Venus as revealed by the Venera landings: Part II: Geological Society of
193 America Bulletin, v. 96, p. 137–144, https://doi.org/10.1130/0016-
194 7606(1985)96<137:TSOVAR>2.0.CO;2.
195 Campbell, B. A., Morgan, G. A., Whitten, J. L., Carter, L. M., Glaze, L. S., and Campbell, D. B.,
196 2017, Pyroclastic flow deposits on Venus as indicators of renewed magmatic activity: Journal
197 of Geophysical Research: Planets, v. 122, p. 1580–1596,
198 https://doi.org/10.1002/2017JE005299.

199 Campbell, I. H., and S. R. Taylor, 1983, No water, no granites - No oceans, no continents:
200 Geophysical Research Letters, v. 10, p. 1061–1064,
201 https://doi.org/10.1029/GL010i011p01061.
202 Carvalho, F. P., Oliveira, J. M., and Soares, A. M. M., 2011, Sediment accumulation and
203 bioturbation rates in the deep Northeast Atlantic determined by radiometric techniques: ICES
204 Journal of Marine Science, v. 68, p. 427–435, https://doi.org/10.1093/icesjms/fsr005.
205 Cofrade, G., Mendiburu-Eliçabe, M., and Romeo, I., 2019, Circular troughs in tessera terrain on
206 Venus: Morphometry, structural analysis and possible formation model: Planetary and Space
207 Science, v. 178, 104706, https://doi.org/10.1016/j.pss.2019.104706.
208 Craddock, R. A., 2011, Aeolian processes on the terrestrial planets: Recent observations and
209 future focus: Progress in Physical Geography, v. 36, p. 110–124,
210 https://doi.org/10.1177/0309133311425399.
211 Ernst, R. E., 2014, Large Igneous Provinces: Cambridge, Cambridge University Press, 663 pp.
212 Fegley, B., Jr., and Treiman, A. H., 1992, Chemistry of atmosphere-surface interactions on
213 Venus and Mars, *in* Luhmann, J. G., Tatrallyay, M., and Pepin, R. O., eds., Venus and Mars:
214 Atmospheres, Ionospheres, and Solar Wind Interactions, American Geophysical Union,
215 Washington, DC, p. 7–71, https://doi.org/10.1029/GM066p0007.
216 Ford, P. G., and Pettengill, G. H., 1992, Venus topography and kilometer-scale slopes: Journal of
217 Geophysical Research, v. 97, p. 13103–13114, https://doi.org/10.1029/92JE01085.
218 Ghail, R. C., and Wilson, L., 2015, A pyroclastic flow deposit on Venus, *in* Platz, T., Massironi,
219 M., Byrne, P. K., and Hiesinger, H., eds., Volcanism and Tectonism Across the Inner Solar
220 System: Geological Society, London, Special Publication 401, p. 97–106,
221 http://dx.doi.org/10.1144/SP401.1.

Ghent, R., and Hansen, V., 1999, Structural and kinematic analysis of Eastern Ovda Regio, Venus: Implications for crustal plateau formation: Icarus, v. 139, p. 116–136, https://doi.org/10.1006/icar.1999.6085.

Gilmore, M. S., Mueller, N., and Helbert, J., 2015, VIRTIS emissivity of Alpha Regio, Venus, with implications for tessera composition: Icarus, v. 254, p. 350–361, https://doi.org/10.1016/j.icarus.2015.04.008.

Gilmore, M. S., Treiman, A., Helbert, J., and Smrekar, S., 2017, Venus surface composition constrained by observation and experiment: Space Science Reviews, v. 212, p. 1511–1540, https://doi.org/10.1007/s11214-017-0370-8.

Greeley, R., Iversen, J., Leach, R., Marshall, J., White, B., and Williams, S., 1984, Windblown sand on Venus: Preliminary results of laboratory simulations: Icarus, v. 57, p. 112–124, https://doi.org/10.1016/0019-1035(84)90013-7.

Hansen, V. L., 2006, Geologic constraints on crustal plateau surface histories, Venus: The lava pond and bolide impact hypotheses: Journal of Geophysical Research, v. 111, E11010, https://doi.org/10.1029/2006JE002714.

Hansen, V. L., and Willis, J. J., 1996, Structural analysis of a sampling of tesserae: Implications for Venus geodynamics: Icarus, v. 123, 296–312, https://doi.org/10.1006/icar.1996.0159.

Hashimoto, G. L., Roos-Serote, M., Sugita, S., Gilmore, M. S., Kamp, L. W., Carlson, R. W., and Baines, K. H., 2008, Felsic highland crust on Venus suggested by Galileo Near-Infrared Mapping Spectrometer data: Journal of Geophysical Research, v. 113, E00B24, http://doi.org/10.1029/2008JE003134.

Head, J. W., and Wilson, L., 1986, Volcanic processes and landforms on Venus: Theory, predictions, and observations: Journal of Geophysical Research, v. 91, p. 9407–9446, https://doi.org/10.1029/JB091iB09p09407.

Helbert, J., Müller, N., Kostama, P., Marinangeli, L., Piccioni, G., and Drossart, P., 2008, Surface brightness variations seen by VIRTIS on Venus Express and implications for the evolution of the Lada Terra region, Venus: Geophysical Research Letters, v. 35, L11201, doi:10.1029/2008GL033609.11.

Herrick, R. R., Stahlke, D. L., and Sharpton, V. L., 2012, Fine-scale Venusian topography from Magellan stereo data: Eos, v. 93, p. 125–126, https://doi.org/10.1029/2012EO120002.

Ingersoll, A. P., 1969, The runaway greenhouse: A history of water on Venus: Journal of the Atmospheric Sciences, v. 26, p. 1191–1198, https://doi.org/10.1175/1520-0469(1969)026<1191:TRGAHO>2.0.CO;2.

Ivanov, M. A., 2001, Morphology of the tessera terrain on Venus: Implications for the composition of tessera material: Solar System Research, v. 35, p. 1–17, https://doi.org/10.1023/A:1005289305927.

Ivanov, M. A., and Head, J. W., 1996, Tessera terrain on Venus: A survey of the global distribution, characteristics, and relation to surrounding units from Magellan data: Journal of Geophysical Research, v. 101, p. 14,861–14,908, https://doi.org/10.1029/96JE01245.

Ivanov, M. A., and Head, J. W., 2011, Global geological map of Venus: Planetary and Space Science, v. 59, p. 1559–1600, https://doi.org/10.1016/j.pss.2011.07.008.

Li, J., Dong, S., Zhang, Y., Zhao, G., Johnston, S. T., Cui, J., and Xin, Y., 2016, New insights into Phanerozoic tectonics of south China: Part 1, Polyphase deformation in the Jiuling and

Lianyunshan domains of the central Jiangnan Orogen: Journal of Geophysical Research: Solid Earth, v. 121, p. 3048–3080, https://doi.org/10.1002/2015JB012778.

McKinnon W. B., Zahnle, K. J., Ivanov, B. A., and Melosh, H. J., 1997, in Bougher, S. W., Hunten, D. M., and Phillips, R. J. eds., Venus II: Geology, Geophysics, Atmosphere, and Solar Wind Environment: University of Arizona Press, Tucson, AZ, p. 969–1014.

Molinaro, M., Leturmy, P., Guezou, J.-C., Frizon de Lamotte, D., and Eshragi, S. A., 2005, The structure and kinematics of the southeastern Zagros fold-thrust belt, Iran: From thin-skinned to thick-skinned tectonics: Tectonics, v. 24, TC3007, https://doi.org/10.1029/2004TC001633.

Ramsey, J. G., 1967, Folding and Fracturing of Rocks: McGraw-Hill, New York, 568 p.

Reynolds, K., Copley, A., and Hussain, E., 2015, Evolution and dynamics of a fold–thrust belt: The Sulaiman Range of Pakistan: Geophysical Journal International, v. 201, p. 683–710, https://doi.org/10.1093/gji/ggv005.

Romeo, I., and Capote, R., 2011, Tectonic evolution of Ovda Regio: An example of highly deformed continental crust on Venus?: Planetary and Space Science, v. 59, p. 1428–1445, https://doi.org/10.1016/j.pss.2011.05.013.

Selivanov, A. S., Gektin, Yu. M., Naraeva, M. K., Panfilov, A. S., and Fokin, A. B., 1985, Evolution of the Venera 13 imagery, Soviet Astronomy Letters, v. 814, p. 235–236.

Senske, D. A., and Plaut, J. J., 2000, The Tellus region of Venus: Processes in the formation and modification of tessera terrain: Lunar and Planetary Science, v. 31, abstract 1496.

Senske, D. A., and Plaut, J. J., 2009, Geologic evidence for a thick volcanic crust in part of Tellus Tessera, Venus: Lunar and Planetary Science, v. 40, abstract 1707.

Way, M. J., and Del Genio, A. D., 2020, Venusian habitable climate scenarios: Modeling Venus through time and applications to slowly rotating Venus-like exoplanets: Journal of

Geophysical Research: Planets, v. 125, e2019JE006276,

https://doi.org/10.1029/2019JE006276.

FIGURE CAPTIONS

Figure 1. (A) A portion of the Magellan global radar mosaic showing examples in Tellus Tessera of arcuate lineaments (marked by gold arrows). Intra-tessera radar-dark material is marked with blue arrows. (B) A sketch map of these lineaments (teal lines), which tend to differ substantially in strike from linear structures that appear to be extensional fractures (thin black lines). Radar-dark material is shown as tan fill. (C) Topographic data (from Herrick et al., 2012) overlain on radar imagery show how the arcuate lineaments follow local topography; the topographic data have a resolution of 0.6 km/px. All images are in azimuthal equidistant projection, centered at 39.3°N, 81.5°E; the radar look direction in (A) and (C) is from the left.

Figure 2. (A) A portion of the Magellan global radar mosaic with examples of arcuate lineaments (gold arrows) and radar-dark deposits (blue arrows) in Ovda Regio. (B) A sketch map of these lineaments and extensional structures (teal and thin black lines, respectively). Tan fill is radar-dark material. (C) Magellan radar imagery of curving lineaments in Alpha Regio. (D) A sketch map of the scene in (C). (E) A TerraColor NextGen satellite image mosaic of a portion of the Siberian Traps in northern Russia. Exposed lava formations follow topography and show arcuate outcrop patterns (gold arrows). (F) A sketch map of the scene in (E); thin black lines mark extensional fractures, grey fill is vegetation cover, and blue fill corresponds to perched lakes. All images are in azimuthal equidistant projection, centered at (A) 4.6°S, 83.5°E; (C) 22.4°S, 1.6°E; and (E) 69.5°N, 91.7°E. The radar look direction in (A) and (C) is from the left, and the solar illumination in (E) is from the south. The satellite view in (E) is provided by Earthstar Geographics and has a resolution of 15 m/px.

Figure 3. (A) A portion of the Magellan global radar mosaic showing examples of features we interpret as eroded periclinal folds (purple arrows) in Tellus Tessera; arcuate lineaments (gold arrow) and radar-dark deposits (blue arrows) are also shown. (B) A sketch map of the scene in (A); dashed black lines delimit exemplar periclinal folds. (C) Landsat/Copernicus Sentinel-2 satellite image data of a region within the Sulaiman Mountains in western Pakistan, where a sequence of Mesozoic to younger sediments are shortened and periclinal folds (purple arrows) abound. (D) A sketch map of the scene in (C), where prominent, exposed strata and minor fractures are mapped as orange and thin black lines, respectively; several periclinal folds are outlined by dashed black lines. (A) is in azimuthal equidistant projection, centered at 38.5°N, 83.0°E; (C) is in orthographic projection, centered at 31.4°N, 68.4°E. The radar look direction in (A) is from the right, and the solar illumination in (C) is from the southeast. The satellite imagery in (C) is provided by Maxar Technologies/CNES/Airbus and has a resolution of 30 m/px.

Figure 4. A schematic illustration of how a combination of folding and erosion leads to the outcrop patterns we report. (A) A set of horizontal layers (orange arrow) is emplaced. (B) These layers are folded in response to regional horizontal compression (red arrows), forming troughs and ridges. (C) Aeolian action erodes these local highs, exposing the constituent layers (gold arrow) and depositing sediments in the subjacent lows (blue arrow).

Figure 01

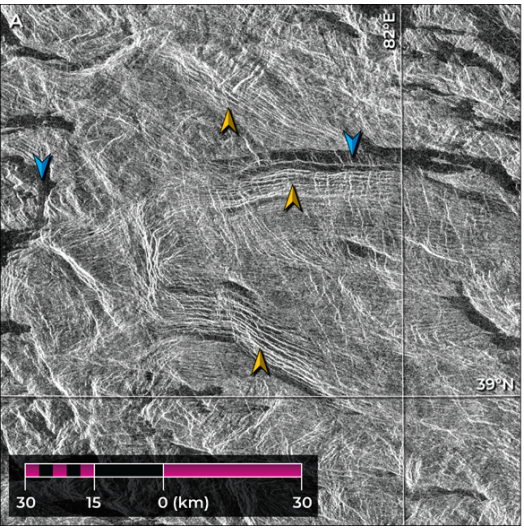
A
82°E
39°N
30
15
0 (km)
30

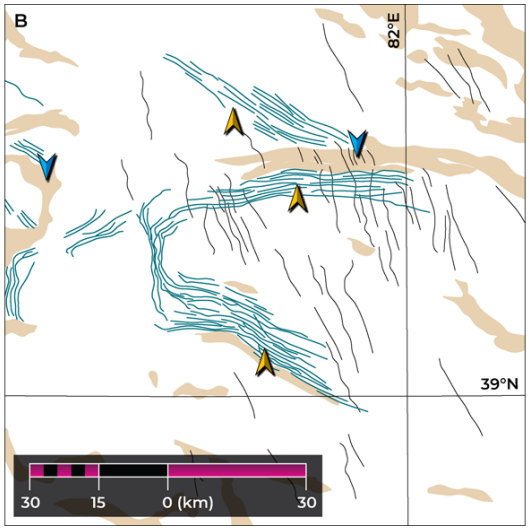
B
82°E
39°N
30
15
0 (km)
30

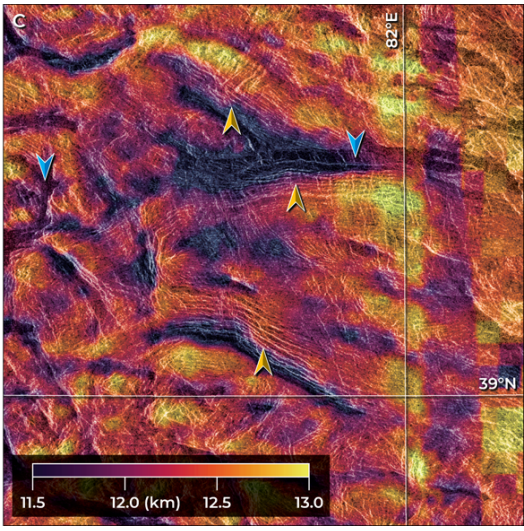
C
82°E
39°N
11.5
12.0 (km)
12.5
13.0

Figure 02

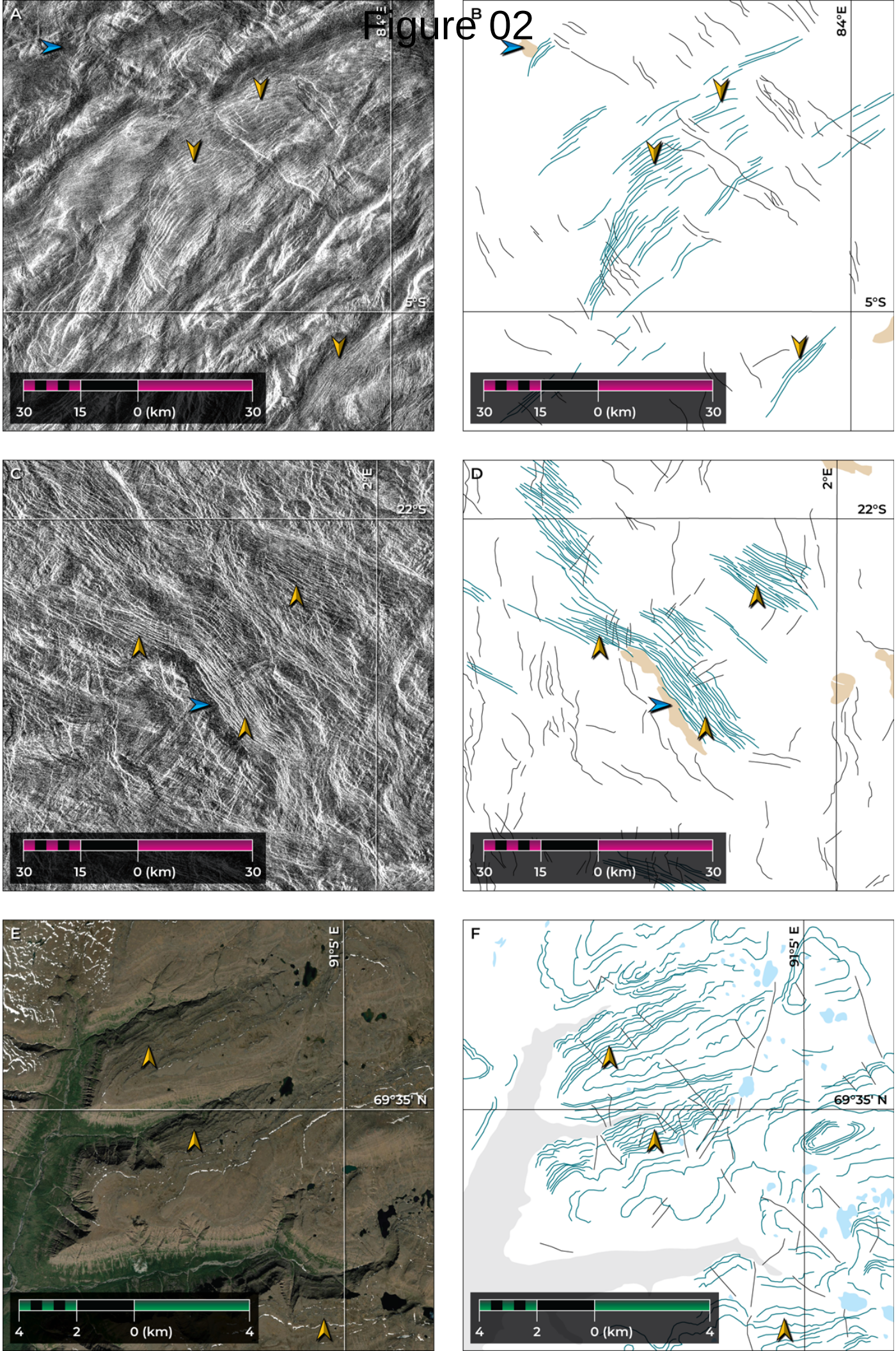
A
84°E
5°S
30
15
0 (km)
30
B
84°E
5°S
30
15
0 (km)
30
C
2°E
22°S
30
15
0 (km)
30
D
2°E
22°S
30
15
0 (km)
30
E
91°5' E
69°35' N
4
2
0 (km)
4
F
91°5' E
69°35' N
4
2
0 (km)
4

Figure 03

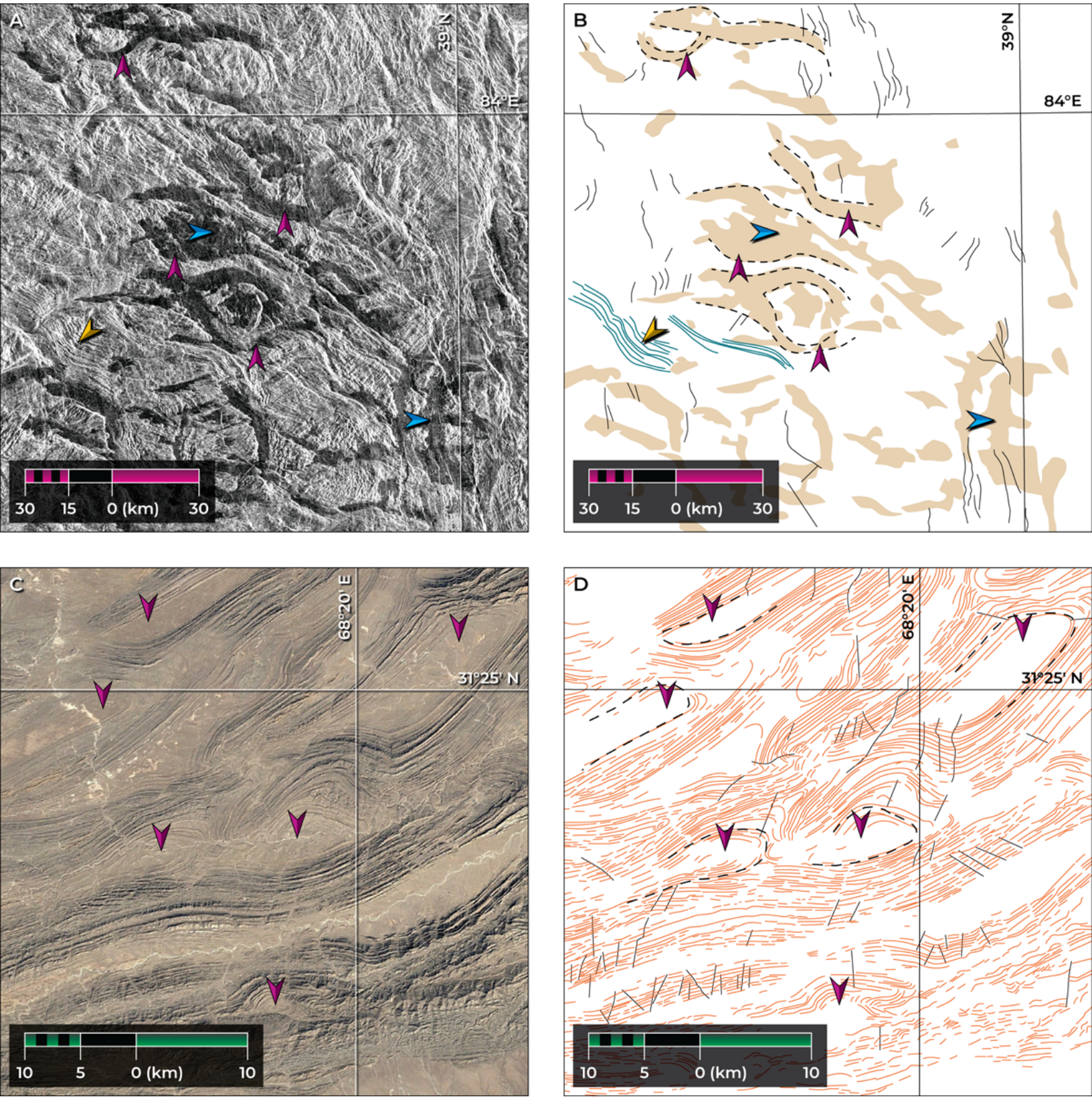
A
39°N
84°E
30 15 0 (km) 30
B
39°N
84°E
30 15 0 (km) 30
C
68°20' E
31°25' N
10 5 0 (km) 10
D
68°20' E
31°25' N
10 5 0 (km) 10

Figure 04